RESEARCH ARTICLE

A radiator-free pressure-to-enthalpy cascade lifts thermal rockets above their wall-temperature limit

New York General Group, Inc.

17 November 2026

A radiator-free pressure-to-enthalpy cascade lifts thermal rockets above their wall-temperature limit

New York General Group, Inc.
17 November 2026

Abstract

Rockets that heat propellant through a solid wall (nuclear-thermal, solar-thermal, beamed-thermal, resistojet) are taken to be bounded by the wall temperature T_w; for hydrogen at 2,800 K this gives a specific impulse near 900 s. Here we show that T_w is not the thermodynamic bound. For any device fed by heat from surfaces no hotter than T_w, with no heat rejection and no net shaft work, the propellant quantity $b_w = h_0 - T_w s$ cannot increase. Stagnation pressure can therefore be traded for stagnation enthalpy above the wall value, and the attainable temperature ratio has a square-root singularity at zero pressure sacrifice. We then ask whether wave rotors can realize this trade. We prove that a matched single-shock wave cycle always consumes more driver gas than it compresses, by a factor $\mu = (\rho_D/\rho_1)/(1 + M_D) > 1$. An engine in which one stream is successively driver and driven gas must therefore split the reheated stream and remix it. For this split-charge cascade, with hydrogen at T_w = 2,800 K, the model predicts about 1,010 s with one rotor (chamber pressure about 65 bar) and about 1,055 s with two rotors (about 32 bar), assuming equilibrium nozzle flow. With chemistry frozen from the chamber the figures are about 970 s and 985 s, against 889 s for the conventional engine. No radiator or hot-gas turbomachinery is involved. The low-pressure part of the wave cycle, leakage, and engine mass remain unresolved.

Main

The wall-temperature limit

The exhaust velocity of a thermal rocket is fixed by the stagnation enthalpy h_0 delivered to the nozzle,

$$I_{sp} = \frac{\lambda}{g_0}\sqrt{2h_0}, \qquad (1)$$

where λ lumps finite area ratio and nozzle losses. In solid-core nuclear thermal propulsion, hydrogen leaves the fuel at 2,550–3,000 K and yields about 900 s (ref. 1). Efforts to raise this figure have targeted the fuel material, or have bypassed the wall with liquid or gaseous cores, pulsed heating (ref. 2), or electrical re-addition of turbine work (refs 3, 4).

A separate line of work places a wave rotor between reactor and nozzle. The wave-rotor-enhanced nuclear (WREN) concept is reported to couple a four-port wave rotor to a closed Brayton cycle, with radiators. Its authors quote 1,400–1,500 s for hydrogen, and 1,200–2,000 s in a bimodal study (refs 5, 6). We take that work as the closest prior art.

We ask a different question. What is the highest stagnation enthalpy that heat from a wall at T_w can deliver when no heat is rejected at all, and can a wave machine deliver it?

A bound that replaces the wall limit

Consider the propellant between station 1 (stagnation state T_w, P_H, reached by ordinary heating) and the nozzle inlet c. The control volume is steady in the cycle-averaged sense. It receives heat q only from surfaces at local temperature $T_b \le T_w$ with $\delta q \ge 0$. It exchanges no net shaft work and rejects no heat. Energy and entropy balances give

$$h_{0c} - h_{01} = q, \qquad s_c - s_1 = \int \frac{\delta q}{T_b} + \sigma \;\ge\; \frac{q}{T_w}, \quad \sigma \ge 0.$$

Eliminating q,

$$b_w(c) \le b_w(1), \qquad b_w \equiv h_0 - T_w s. \qquad (2)$$

This is the availability inequality referred to the wall instead of the environment. Since $(\partial h/\partial s)_P = T$, it has a simple geometric form on an enthalpy–entropy chart. The reachable states lie on or below the tangent to the isobar P_H at the wall state (Fig. 1b). Every lower isobar crosses that tangent above the wall enthalpy.

For a perfect gas with $\kappa = R/c_p$, $\tau = T_{0c}/T_w$ and $x = P_c/P_H$,

$$\tau - 1 - \ln\tau \;\le\; \kappa \ln\frac{1}{x}, \qquad (3)$$

$$\tau_{\max}(x) = -W_{-1}\!\left(-\frac{x^{\kappa}}{e}\right), \qquad (4)$$

where W_{-1} is the lower real branch of the Lambert function. A conventional engine sits at $x = 1$, $\tau = 1$. Near that point,

$$\tau_{\max} - 1 \approx \sqrt{2\kappa \ln(1/x)}, \qquad (5)$$

so $d\tau_{\max}/dx \to -\infty$ as $x \to 1$. The first increment of pressure sacrificed buys the most temperature (Table 1).

Table 1 | Ideal bound of equation (4), perfect gas, κ = 0.234

P_c/P_H	$\tau_{\max}$	Ideal I_{sp} gain, $\sqrt{\tau_{\max}}$
0.9	1.24	1.11
0.7	1.47	1.21
0.5	1.68	1.30
0.3	1.95	1.40
0.1	2.42	1.56

The energy comes from the reactor, not from the pump. Pressure supplies low entropy, which lets the gas absorb additional heat at T_w and carry it as work.

If the control volume is extended back to the cold pump exit at $T_{in} = \theta T_w$, the same argument gives an outer envelope,

$$\tau - 1 - \ln\tau \;\le\; (\theta - 1 - \ln\theta) + \kappa \ln\frac{1}{x}. \qquad (6)$$

For $\theta = 0.1$ and $x = 1$ this allows $\tau \approx 3.7$. Reaching it would require reversible use of the cold propellant as a heat sink, which we do not pursue.

Why work must be exchanged

Convective heating alone cannot approach (4). Heat flows from wall to gas only while T_w exceeds the recovery temperature, so

$$\frac{T_0}{T_w} \le \frac{1+\frac{\gamma-1}{2}M^2}{1+r\,\frac{\gamma-1}{2}M^2} < \frac{1}{r}, \qquad (7)$$

with recovery factor $r \approx 0.9$ for turbulent flow. The gain is at most about 10%, and only at high Mach number.

The process that saturates (3) is isothermal expansion at T_w, absorbing heat and producing work, followed by adiabatic recompression of the same gas with that work. Consider an ideal counter-current exchanger with N expansion steps of overall ratio $\pi = P_H/P_L$ and a reheat to T_w after each. Let η_e be the expansion efficiency. Let η_c be the ratio of the isentropic enthalpy rise corresponding to the achieved pressure ratio to the actual enthalpy rise. Then

$$\tau_N = 1 + N\eta_e\left(1-\pi^{-\kappa/N}\right) \xrightarrow{N\to\infty} 1+\eta_e\,\kappa\ln\pi, \qquad (8)$$

$$\frac{P_c}{P_H} = \frac{1}{\pi}\Big[1+\eta_c(\tau_N-1)\Big]^{1/\kappa}. \qquad (9)$$

With $\eta_e = \eta_c = 1$ and $N \to \infty$, (8) and (9) reproduce the equality in (3). The bound is therefore attainable in principle. Bladed machines cannot work at 2,800 K. Wave rotors exchange work directly between gas streams, and their passages see hot and cooler gas alternately (refs 7–9). The question is what a real wave cycle can deliver.

A mass-ratio law for matched wave cycles

We analysed the high-pressure part of a through-flow cycle exactly, for a perfect gas with γ = 1.3 (Fig. 1c, Methods). The sequence is as follows.

1. A passage holds charge gas at rest at $p_1 = P_L$, $T_1 = T_w$.
2. Its inlet end opens to driver gas at stagnation state (P_H, T_w). A shock of Mach number M_s runs into the charge.
3. When the shock reaches the far end, the delivery port opens at the matched post-shock pressure. Shocked charge leaves at uniform state.
4. The driver port closes early. The resulting expansion reaches the delivery end exactly when the driver–charge interface does, and the delivery port closes.

All states in this part are uniform and are joined by one shock, one interface and centred expansions. The delivered charge has stagnation-enthalpy ratio

$$\tau_s = \frac{T_2}{T_1} + \frac{\gamma-1}{2}\left(\frac{u_2}{a_1}\right)^2.$$

For subsonic or sonic admission, the ratio of driver mass admitted to charge mass delivered is

$$\mu \equiv \frac{m_D}{m_d} = \frac{\rho_D/\rho_1}{1+M_D}, \qquad \mu - 1 \approx (\gamma-1)M_D \;\; (M_D \ll 1), \qquad (10)$$

where ρ_D and M_D are the density and Mach number of the admitted driver gas behind the interface. The driver enters denser than the charge because it is at higher pressure and has cooled on expansion. Hence $\mu > 1$ at every finite pressure ratio. A matched single-shock cycle cannot process equal masses of driver and charge.

Energy conservation then fixes the work extracted per unit driver mass, and with it the best exhaust state:

$$\frac{w}{c_pT_w} = \frac{\tau_s-1}{\mu}, \qquad \mathcal{M} \equiv \frac{P_{X,\max}}{P_L} = \pi\left(1-\frac{\tau_s-1}{\mu}\right)^{\gamma/(\gamma-1)}. \qquad (11)$$

$P_{X,\max}$ is the stagnation pressure the driver exhaust would have if only the incident shock were dissipative. The exhaust must return through the reheat pass to P_L, so the cycle closes only if the realized exhaust pressure exceeds $P_L/(1-\delta)$, where δ is the fractional loss of that pass. We call $\mathcal{M}$ the closure margin.

Table 2 | Matched single-shock cycle, perfect gas, γ = 1.3

$\pi = P_H/P_L$	p_2/p_1	M_s	τ_s	P_{0s}/P_L	μ	w/c_pT_w	η_w	$\mathcal{M}$
2.0	1.75	1.29	1.173	1.96	1.24	0.140	0.94	1.04
3.0	2.24	1.45	1.286	2.81	1.43	0.201	0.90	1.14
5.54	3.03	1.67	1.467	4.53	1.74	0.269	0.82	1.43
10	3.87	1.88	1.663	6.88	2.14	0.309	0.75	2.01
30	≈5.9	≈2.30	≈2.12	≈14	≈3.4	≈0.33	≈0.60	≈5.4

P_{0s} is the stagnation pressure of the delivered charge. η_w is w divided by the isentropic work of expansion through π.

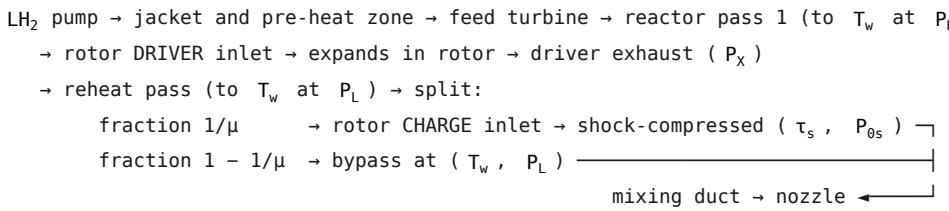
Three results follow.

- **Sonic admission.** At π = 5.54 the driver enters exactly at Mach 1. Above it the port is choked and the driver enters through an attached expansion.
- **Saturation.** The work per unit driver mass saturates near 0.31–$0.33\,c_pT_w$ beyond $\pi \approx 10$. Higher admission ratios raise $\mathcal{M}$, not the work.
- **Closure.** Below $\pi \approx 3$ the margin is too small to pay for any realistic reheat-pass loss.

The split-charge wave cascade

Because $\mu > 1$, only the fraction $1/\mu$ of the reheated stream can re-enter the rotor as charge. The engine of Fig. 1a therefore works as follows.

Fig. 1a | Flow path, one rotor.



All propellant passes through pass 1, the rotor's driver side and the reheat pass. The compressed charge is the primary stream of a mixing duct that entrains the bypass. The rotor is adiabatic and the mixing duct conserves stagnation enthalpy. The chamber enthalpy is therefore

$$h_{0c} = h(T_w, P_L) + w,$$

independent of how the pressure is recovered. Rotor and mixing losses fall on P_c and on w, never on the accounting of energy.

The bypass can instead drive a second rotor at a lower pressure level, whose own exhaust is reheated and split again. With N such levels at equal admission ratio,

$$w_{tot} = w \sum_{k=0}^{N-1} \left(1 - \frac{1}{\mu}\right)^k, \qquad \text{final bypass fraction} = \left(1 - \frac{1}{\mu}\right)^N. \qquad (12)$$

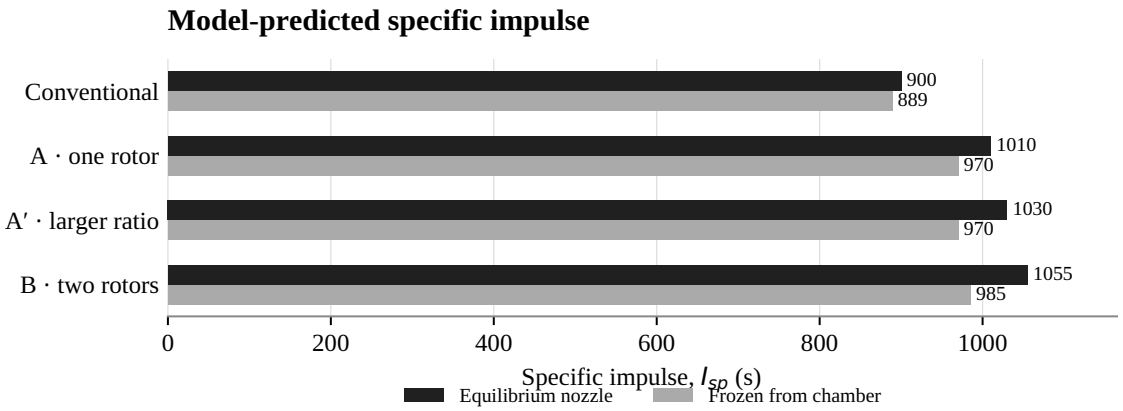
Predicted performance

We evaluated hydrogen with tabulated enthalpy and entropy and equilibrium dissociation at every station (Methods; ref. 10). Wave-level quantities from Table 2 were applied to the real-gas isentropic work. A factor ζ multiplies the exchanged work to represent leakage, friction and wall heat exchange in the rotor; ζ = 0.85 is an assumption, not a

measurement. The reference thrust is 111 kN. $\lambda = 0.923$ was calibrated so that the conventional engine returns 900 s with equilibrium nozzle flow.

Table 3 | Model predictions, hydrogen, T_w = 2,800 K, ζ = 0.85

	Conventional	A: one rotor	A′: one rotor, larger ratio	B: two rotors
Pressure levels (bar)	70	200 / 36	200 / 20	250 / 45 / 8.1
Admission ratio per rotor	–	5.54	10	5.54
μ	–	1.74	2.14	1.74
Flow shock-compressed / bypassed	–	0.58 / 0.42	0.47 / 0.53	0.82 / 0.18
Work exchanged, ideal waves (MJ kg⁻¹)	0	13.5	15.4	19.2
Work exchanged, ζ = 0.85 (MJ kg⁻¹)	0	11.4	13.1	16.3
h_{0c} (MJ kg⁻¹, from 0 K gas)	45.7	57.5	59.7	63.0
Chamber pressure (bar)	70	≈65	≈35	≈32
Chamber temperature (K)	2,800	≈3,250	≈3,270	≈3,350
Dissociated fraction	0.5%	≈2.0%	≈2.8%	≈3.6%
I_{sp}, equilibrium nozzle (s)	900	≈1,010	≈1,030	≈1,055
I_{sp}, frozen from chamber (s)	≈889	≈970	≈970	≈985
Mass flow (kg s⁻¹)	12.6	11.2	11.0	10.7
Reactor power (MW)	≈575	≈645	≈655	≈675
Share of power in reheat	0	21%	24%	28%
Pump discharge (bar)	≈90	≈320	≈320	≈420



The gain over the conventional engine is 12–17% with equilibrium nozzle flow and 9–11% if recombination froze at the chamber. The true value lies between these; a finite-rate nozzle calculation is needed to place it. Designs A and B realize about 30% of the excess enthalpy that (4) permits at their own P_c/P_H.

Table 4 | Sensitivity of Design A (P_H = 200 bar)

Case	ζ	π	P_L (bar)	P_c (bar)	I_{sp}, equilibrium (s)
Nominal	0.85	5.54	36	≈65	≈1,010
Ideal waves	1.00	5.54	36	≈65	≈1,030
Poor rotor	0.70	5.54	36	≈60	≈990
Closure needs $\mathcal{M}$ = 2	0.85	10	20	≈35	≈1,030
Closure needs $\mathcal{M}$ = 2, poor rotor	0.70	10	20	≈33	≈1,010

Specific impulse is insensitive to rotor quality and to pressure losses. What these degrade is chamber pressure.

Pressure closure and the reheat pass

The low level is not imposed; it floats. If the realized exhaust pressure cannot pay for the reheat-pass loss at a given P_L, the periodic state settles at a lower P_L, hence a larger π and a larger margin. Table 4 shows the consequence: P_c falls roughly in proportion and I_{sp} does not fall.

Two effects consume the margin.

- **Reheat-pass loss.** The pass raises the gas only from about 2,200 K to 2,800 K, so its channels can be short (length-to-diameter ratio near 200). At an exit Mach number of 0.15 we estimate $\delta \approx 0.08$–0.10, mostly friction; the loss scales with the square of the Mach number.
- **Non-uniform exhaust.** The part of the driver gas pushed out by incoming charge leaves with a stagnation pressure only 7–17% above P_L for scavenging Mach numbers of 0.5–0.8. The part that leaves during blow-down has more. How much a real collector recovers is not resolved here.

At π = 5.54 the ideal margin of 1.43 must cover both. We consider it likely, but not established, that Design A closes as tabulated; A′ shows the fallback.

The flow area of the reheat pass is the main reactor penalty. At 36 bar and Mach 0.15–0.2 it is 0.047–0.062 m², against about 0.021 m² for the conventional core at Mach 0.25. Allowing for the shorter channels, the reheat zone has a volume comparable to a conventional fuel zone while carrying one-fifth of the power. In Design B the 8-bar pass needs about 0.11 m² for 42% of the flow. Raising all pressures in proportion shrinks these areas and raises pump pressure.

Feed system

The hot gas path contains no turbomachinery, but the engine needs a liquid-hydrogen pump. With 10% loss in pass 1, 10% in jacket and lines, and a full-flow feed turbine of pressure ratio 1.3–1.35, the pump discharge is about 320 bar (A) and 420 bar (B). With pump efficiency 0.70 the shaft work is 0.6–0.8 MJ kg⁻¹, or 7–8 MW, about 1.2% of reactor power. The upper figure is near the roughly 450 bar of the most demanding flight hydrogen pump (ref. 11).

A full-flow turbine of efficiency 0.8 balances this only if its inlet is at about 700 K (A) or 800 K (B). Heating all the propellant to that level takes 10–11 MJ kg⁻¹, about one-sixth of reactor power. Passive pickup in nozzle and reflector is too small. The engine therefore needs a dedicated pre-heat zone ahead of the turbine, or a hotter partial-flow turbine. The turbine work returns to the propellant, so there is no direct I_{sp} penalty.

Feasibility of the wave machine in hot hydrogen

Rotor speed. A passage of width w_p must open in a time short compared with the wave transit time L/a, so $\varepsilon_o = w_p a/(UL)$ must be small. The gas must also exchange little heat with the walls, so NTU $\approx 2\,\mathrm{St}\,L/w_p$ must be small. Their product is independent of geometry:

$$\varepsilon_o \cdot \mathrm{NTU} = \frac{2\,\mathrm{St}\,a}{U}. \qquad (13)$$

In hydrogen at 2,800 K, $a \approx$ 3,860 m s⁻¹. With St ≈ 0.0025, keeping $\varepsilon_o \approx$ NTU ≈ 0.28 requires a passage speed $U \approx$ 250 m s⁻¹. The stress scale $\rho_s U^2$ is then about 120 MPa for carbon–carbon and 1.2 GPa for tungsten. Equation (13) excludes refractory metals and points to coated carbon–carbon.

Internal heat leak. Shocked charge at about 1.34 T_w gives heat to the passage wall, and the cooler driver gas takes it back. This short-circuits part of the exchanged work. A shocked parcel travels on average half the passage, so the fraction lost is about $\frac{1}{2}\mathrm{NTU}\,(T_2 - T_m)/(T_{02} - T_w) \approx 0.10$ for a wall at mean temperature $T_m \approx T_w$. Boundary layers that restart behind each shock transfer more heat than the steady correlation predicts. If St doubles, the loss is about 0.20. The nominal ζ = 0.85 thus leaves little for leakage, and ζ = 0.70 is a credible outcome.

Indicative rotor for Design A. Mean radius 0.15 m, passage height 0.04 m, length 0.6 m, about 75 passages of 11 mm width, four cycles per revolution, about 16,000 r.p.m. These follow from continuity, a cycle period of six acoustic transits and equation (13); they are not a design. The driver port then spans only about two passage widths. Finite-opening losses will therefore be larger than in air machines, and narrowing the passages raises the heat leak by (13).

Thermal and chemical state. Passages see gas between about 1,700 K (expanded driver) and 3,400 K (shocked charge) at roughly 1 kHz. We estimate a surface temperature ripple of order 100 K. Carbon reacts with hot hydrogen to form hydrocarbons, so a carbide coating (ZrC, NbC or TaC) is required. Its expansion mismatch with the substrate, under kilohertz thermal cycling and 120 MPa hoop stress, makes spallation the leading material risk.

System consequences

For a velocity increment of 6 km s^{-1} the propellant fraction falls from 0.49 (900 s) to 0.45 (A) and 0.44 (B). At fixed mass ratio the velocity increment rises by 12% and 17%.

The engine will be heavier. For fixed payload and velocity increment Δv, initial mass is unchanged when the burnout mass M_f grows by

$$\frac{\Delta m_e}{M_f} = \exp\left(\frac{\Delta v}{c_0} - \frac{\Delta v}{c_1}\right) - 1, \qquad (14)$$

where c_0 and c_1 are the exhaust velocities without and with the cascade. At 6 km s^{-1} this is 7.7% (A) and 10.5% (B), before credit for smaller tanks. For a 70-t burnout mass the break-even is 5.4 t and 7.4 t across all engines.

We have no mass estimate for the rotor, hot ducts and mixing duct. The reheat zone alone could add of order 1 t per 111-kN engine, against a conventional engine mass of roughly 3–3.5 t (ref. 1). A net benefit at vehicle level is therefore plausible for Design A but not demonstrated. For Design B it depends on shrinking the low-pressure reheat zone.

If the rotor is bypassed, the engine reverts to conventional operation at 900 s. The bound and the cascade apply unchanged to solar-thermal, beamed-thermal and resistojet engines.

Relation to earlier work and limits of this study

Wave-rotor superheating of reactor-heated hydrogen has been proposed in WREN with a closed Brayton loop (refs 5, 6). Recycling of turbine work into the propellant has been proposed with induction or electromagnetic heating (refs 3, 4). Reverse-flow pressure-wave machines with near-equal mass flows have operated in air (ref. 7). Our claims are:

- the bound (2)–(6), its tangent construction and its singular behaviour (5);
- the mass-ratio law (10) and the closure margin (11);
- the split-charge topology, with no closed loop and no heat rejection, and its nested form (12);
- the speed law (13).

Four things are not established.

- **The low-pressure part of the cycle.** Blow-down, scavenging and recharge were treated only through cycle-integrated mass and energy balances and the ideal margin (11). A time-accurate one-dimensional computation of the periodic state, with finite opening and leakage, is the necessary next step. It would fix the realized margin and ζ.
- **Leakage.** End gaps separate gas at up to 200 bar from gas at 36 bar.
- **Nozzle chemistry.** The two bounds in Table 3 differ by 4–7%.
- **Mass.** See above.

Our comparison with WREN rests on its published summaries; overlap in details cannot be excluded. An electrically heated hydrogen rotor test at reduced scale would address the first two items directly.

Methods

Thermodynamic data. H_2 enthalpy and entropy and the equilibrium constant of $H_2 \rightleftharpoons 2H$ were taken from the NIST–JANAF tables (ref. 10) and interpolated linearly in T (enthalpy, entropy) or $1/T$ ($\log_{10} K_p$).

- $H(T) - H(298\ \mathrm{K})$ = 39.5, 46.2, 53.0, 70.5, 88.7, 107.6 kJ mol^{-1} at 1,600, 1,800, 2,000, 2,500, 3,000, 3,500 K, and 81.4 at 2,800 K.
- $H(298\ \mathrm{K}) - H(0)$ = 8.47 kJ mol^{-1}.
- S° = 180.9, 184.8, 186.7, 188.4 J mol^{-1} K^{-1} at 1,600, 1,800, 1,900, 2,000 K, and 200.3 at 2,800 K.

- $\log_{10} K_p$ = −1.61, −0.46, 0.40 at 3,000, 3,500, 4,000 K, and −2.19 at 2,800 K by extrapolation.
- Dissociated fraction $\alpha \approx \sqrt{K_p/4P}$; dissociation enthalpy 460 kJ mol^{-1}.
- Wall-state enthalpies including dissociation: 45.7, 45.2, 46.1, 46.6 MJ kg^{-1} at 70, 200, 36, 20 bar.

Interpolation and the small-α approximation limit the accuracy of enthalpies to about 1% and of I_{sp} ratios to about 0.5%. An independent check with a standard equilibrium code is advisable.

Isentropic work. End states from $S^\circ(T_2) = S^\circ(T_1) - R\ln\pi$. For π = 5.54: 1,867 K, 33.0 kJ mol^{-1} (16.35 MJ kg^{-1}). For π = 10: 1,613 K, 41.4 kJ mol^{-1} (20.5 MJ kg^{-1}). Exchanged work is $\zeta\,\eta_w$ times these, with frozen composition in the expansion.

Wave cycle. Perfect gas, γ = 1.3, instantaneous ports, $p_1 = P_L$, $T_1 = T_w$. Velocities are in units of a_1, times in L/a_1.

- Shock: $p_2/p_1 = 1 + \frac{2\gamma}{\gamma+1}(M_s^2 - 1)$; $u_2 = \frac{2}{\gamma+1}(M_s - 1/M_s)$; $T_2/T_1 = \frac{[2\gamma M_s^2 - (\gamma-1)][(\gamma-1)M_s^2+2]}{(\gamma+1)^2 M_s^2}$.
- Subsonic admission: $T_D/T_w = 1 - \frac{\gamma-1}{2}u_2^2$; $P_H/p_2 = (T_w/T_D)^{\gamma/(\gamma-1)}$.
- Choked admission (π > 5.54): sonic state at the port followed by an attached centred expansion, $u_2 + \frac{2a_D}{\gamma-1} = \frac{\gamma+1}{\gamma-1}a^*$, $p_2/p^* = (a_D/a^*)^{2\gamma/(\gamma-1)}$.
- Driver-port closing time t_c follows from requiring the head of the closing expansion to meet the interface at $x = L$. For $M_D \le 1$, $t_c = \frac{L}{u_2}\frac{a_D}{u_2 + a_D}$, which gives (10). For choked admission the head was integrated through the attached expansion and the admitted mass taken as sonic flux times t_c.
- Design A coordinates: shock $x = 1.671t$, arriving at 0.598; interface $x = 0.9325t$, arriving at 1.072; driver port closes at 0.536; delivery port open from 0.598 to 1.072. Delivered mass equals $\rho_1 L$ to within 0.1%.

Mixing duct. Constant-area mixing of two perfect-gas streams with equal static pressure at entry, solved from mass, momentum and energy for the subsonic mixed state. The delivered charge was assumed to retain 88% of P_{0s}. Results: $P_c \approx 1.8P_L$ (A), $1.75P_L$ (A′), and two successive mixings giving $3.9P_L$ (B). Chemistry in the duct was not modelled.

Chamber state. Solved from $H_{\text{frozen}}(T) + \alpha(T,P)\,\Delta H_d = H_{\text{total}}$.

Specific impulse. Equation (1) with λ = 0.923 for the equilibrium case. The frozen bound multiplies this by $\sqrt{1 - \alpha_c \Delta H_d / H_{\text{total}}}$, which neglects the change in expansion exponent.

Reheat pass. Density from the ideal-gas law at exit conditions. Friction loss $4f(L/D)\,\gamma M^2/2$ with f = 0.005, plus heat-addition loss $\frac{1}{2}\gamma M^2 \ln(T_{out}/T_{in})$ and two dynamic heads for turning and entry.

Feed system. Liquid density 75–77 kg m^{-3} averaged over the pressure rise; turbine gas c_p = 14.7 kJ kg^{-1} K^{-1}, γ = 1.4.

Rotor. St from $0.023\,Re^{-0.2}Pr^{-2/3}$. Surface ripple from the semi-infinite-solid response to a heat-flux pulse, with effusivity 1.2×10^4 J m^{-2} K^{-1} s$^{-1/2}$.

Figure legend

Fig. 1 | Bound, flow path and wave cycle. a, Flow path of the one-rotor engine (shown above as a schematic). **b**, Enthalpy–entropy chart of hydrogen. The straight line of slope T_w tangent to the isobar P_H at the wall state is the bound (2). The conventional engine is the tangent point. Designs A and B lie between the wall isotherm and the tangent, on the isobars P_c. **c**, Position–time chart of the high-pressure part of the cycle for Design A, showing the shock, the driver–charge interface, the closing expansion and the port timings listed in Methods.

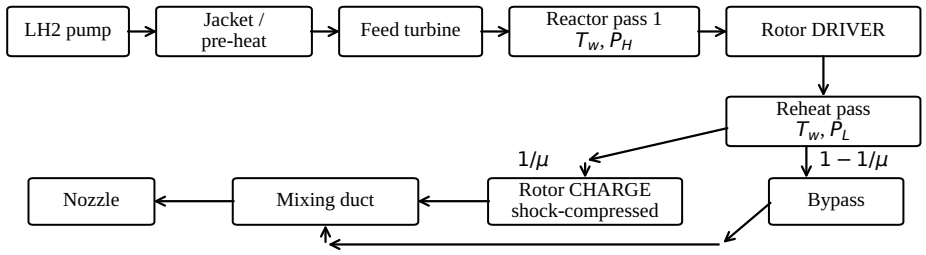
Data availability

All inputs are given in Methods. No datasets were generated.

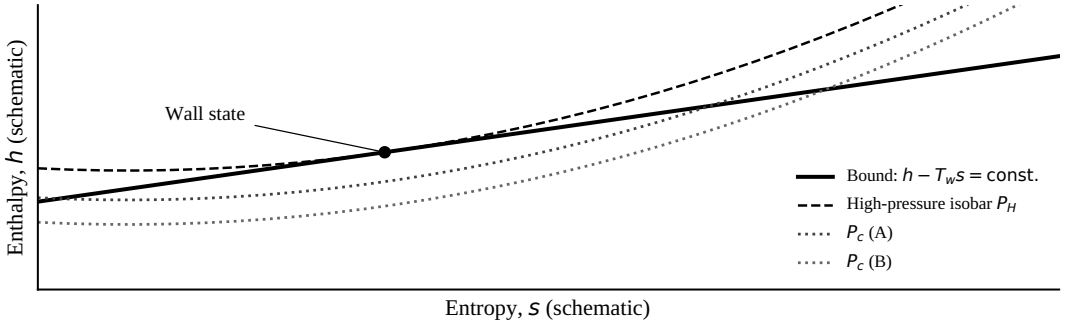
References

1. Borowski, S. K., McCurdy, D. R. & Packard, T. W. Nuclear thermal propulsion (NTP): a proven growth technology for human NEO/Mars exploration missions. *IEEE Aerospace Conf.* (2012).
2. Arias, F. J. On the use of a pulsed nuclear thermal rocket for interplanetary travel. *52nd AIAA/SAE/ASEE Joint Propulsion Conf.* (2016).
3. Dujarric, C., Santovincenzo, A. & Summerer, L. The nuclear thermal electric rocket: a proposed innovative propulsion concept for manned interplanetary missions. *4th Eur. Conf. for Aerospace Sciences (EUCASS)*

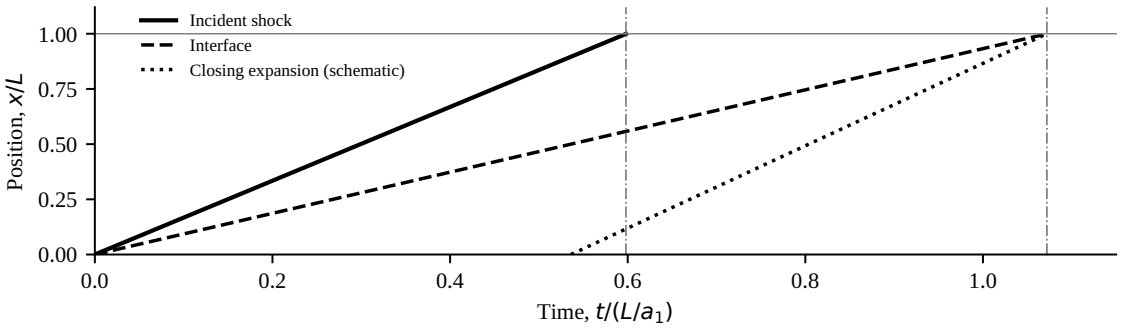
a Split-charge engine: one-rotor flow path



b Wall-referenced enthalpy–entropy bound (schematic)



c Position–time diagram: Design A



(2011).
4. Tymczak, C. J. Nuclear thermo-electric thruster. Preprint at https://arxiv.org/abs/2401.03344 (2024).
5. Gosse, R. C. et al. Nuclear wave rotor bi-modal cycle for in-space propulsion. *AIAA SciTech 2024 Forum*, AIAA 2024-1238 (2024).
6. Osborne, G. & Gosse, R. Influence of wave rotor thermal decomposition on alternative nuclear rocket propellant performance. *Energies* **19**, 4047 (2026).
7. Akbari, P., Nalim, R. & Mueller, N. A review of wave rotor technology and its applications. *J. Eng. Gas Turbines Power* **128**, 717–735 (2006).
8. Wilson, J. & Paxson, D. E. Wave rotor optimization for gas turbine engine topping cycles. *J. Propul. Power* **12**, 778–785 (1996).
9. Kentfield, J. A. C. *Nonsteady, One-Dimensional, Internal, Compressible Flows* (Oxford Univ. Press, 1993).
10. Chase, M. W. *NIST–JANAF Thermochemical Tables* 4th edn (American Institute of Physics, 1998).
11. Sutton, G. P. & Biblarz, O. *Rocket Propulsion Elements* 9th edn (Wiley, 2017).